Kinetic Study of Torrefied Woody Biomass *via* TGA Using a Single Heating Rate and the Model-Fitting Method

Chang-Goo Lee, Min-Ji Kim, and Chang-Deuk Eom *

A model-fitting method at a single heating rate (10 °C·min^{-1}) was used to investigate the thermal kinetic characteristics of torrefied woody biomass. The kinetic parameters were examined for pine, oak, and bamboo samples with the order of the reaction set ranging from 0.1 to 0.5 and 1.0. Based on the thermogravimetric, derivative thermogravimetric, and derivative^2 thermogravimetric curves obtained, the ranges at which substantial hemicellulose and cellulose pyrolysis occurs were set as the analysis range, and the kinetic parameters of each species were analyzed. The activation energy and pre-exponential factor were obtained at these analytical ranges using two differential methods (Friedman and Chatterjee-Conard) and an integral method (Coats-Redfern). Although there were numerical differences between the results of the differential and integral methods, the thermal properties of each sample exhibited a consistent trend. Softwood was found to have the highest reactivity and intermolecular collisions per unit weight during thermal decomposition. In the case of the torrefied oak and torrefied bamboo, considering that the carbon content and fixed carbon content were approximately 24% to 25% higher than the softwood, it is appropriate to consider the thermal characteristics of each species for producing a solid fuel based on the application.

DOI: 10.15376/biores.17.1.411-428

Keywords: Torrefied biomass; Kinetics; Single heating rate; Differential and integral methods; Activation energy; Pre-exponential factor

*Contact information: Division of Wood Industry, Department of Forest Products and Industry, National Institute of Forest Science, Seoul 02455 Republic of Korea; * Corresponding author: willyeom@korea.kr*

INTRODUCTION

Research on pretreatments to improve the energy density of biomass has been steadily progressing. Torrefaction, a mild pyrolysis technology, is a pretreatment technique for improving biomass feedstock to be in the same league as coal by its treatment within a reaction temperature range of 200 to 300 °C in an anoxic atmosphere (Stelt *et al.* 2011; Mamvura and Danha 2020). Over a 10-year period, torrefied wood has been introduced as a high-efficiency fuel along with information on its chemical composition (Prins *et al*. 2006; Phanphanich and Mani 2011; Bach and Tran 2015; Chen *et al*. 2018, 2021). As knowledge on the thermal decomposition of biomass is critical for investigating its thermal properties with respects to biomass energy utilization, information on the chemical kinetics of biomass thermal decomposition and the investigation of its reaction mechanism are crucial. Thermogravimetric analysis (TGA), which is commonly used for analyzing the kinetics in a pyrolysis reaction of polymer materials, measures the mass loss of a sample

as a function of the temperature. Kinetic analysis using TGA can be performed under isothermal and nonisothermal conditions, which can also be divided into model-free and model-fitting methods (Vyazovkin and Wight 1999). In the model-free method, the activation energy can be calculated at multiple heating rates without any assumptions on the reaction model (Rana *et al*. 2013). On the other hand, the advantage of this method is that the area can be set for kinetic analysis from the results from TG and derivative TG (DTG), which are obtained from the model-fitting method under a condition of single heating rate. Therefore, the reaction model can be assumed, and the parameters of the reaction kinetics are arbitrarily determined from the thermogravimetric (TG) and derivative TG (DTG) curves at a single heating rate (Jang *et al*. 2020). Studies on the reaction kinetics of woody biomass, *i.e.*, lignocellulosic biomass, have evaluated its fuel efficiency as a solid fuel (Idris *et al*. 2010; Chen *et al*. 2012; El-Sayed and Mostafa 2014, 2015; Saldarriaga *et al*. 2015; Carrier *et al*. 2016). In particular, certain reaction kinetic studies on torrefied woody biomass have reported that the activation energy decreases with increases in the treatment temperature and residence time of torrefaction (Ren *et al*. 2013; Gaitán-Álvarez *et al*. 2018; Barzegar *et al*. 2020). However, in most previous studies, multiple heating rates have primarily been used and the order of the reaction has been arbitrarily set using the model-free method (Wang *et al*. 2018). Although it is beneficial to investigate the overall thermal degradation behavior of the sample through the change in the heating rate using the model-free method, investigation of the thermal degradation behavior of the major components, *i.e.*, cellulose, hemicellulose, lignins, *etc*., of a biomass sample using the model-fitting method at a single heating rate can provide useful data. More specifically, in torrefied wood, the proportion of hemicellulose is very low due to thermal decomposition, and thus, low-concentration hemicellulose is thermally decomposed relatively quickly and converted in the temperature range of thermal decomposition generally assigned to cellulose. It is important to select the proportions of cellulose and hemicellulose in each temperature range of thermal decomposition giving the best response under various conditions of the heating rates. In this study, a kinetic analysis was employed in an effort to demonstrate changes associated with the wood torrefaction process. Focus was placed on the fact that torrefied wood has low hemicellulose proportions in the wood cell wall, and this aspect can be quantified *via* a model-fitting method at the single heating rate.

Therefore, the final objective of this study was to clarify the pyrolysis mechanism of torrefied wood through its kinetics. In addition, a comparative analysis was performed between the equations of the differential and integral kinetics. In this study, the authors focus on the pyrolysis mechanism of cellulose and hemicellulose, while excluding lignins. Lignins, which are a primary component in the wood cell wall, continuously degrade under a wide temperature range from the beginning of pyrolysis to the end. Therefore, the evaluation of the wide range of thermal decomposition temperatures for lignins at a single heating rate is difficult. Hence, the range for lignins was not included in this study because the thermal decomposition parameters cannot be accurately determined.

EXPERIMENTAL

Materials

Samples of *Pinus densiflora* Siebold & Zucc, *Quercus serrata* Thumb. ex Murray, and *Phyllostachys nigra* var. Henosis honda (later referred to as pine, oak, and bamboo, respectively) were used in this study. The pine and oak samples included wood chips for

pulp, and the bamboo was cut to a length of approximately 30 mm. The torrefaction treatment of the samples was performed using a self-made apparatus (also known as a "wood roaster") as described in a previous study by Lee *et al.* (2016). The apparatus was rotated a speed of 45 rpm, while blocking oxygen from the outside. When the internal temperature of the roaster reached 220 °C through the application of direct heat at the bottom of the roaster, the top was opened, and the wooden chip samples were inserted. After 300 s in the roaster, the torrefied materials were removed and crushed. In addition, the torrefied wood powder of each species, including the untreated materials, were passed through a #40 standard sieve, and these samples were used as the experimental material. In this study, the following abbreviations are used: for the untreated samples - untreated pine (UP), untreated oak (UO), and untreated bamboo (UB); for the torrefied samples - torrefied pine (TP), torrefied oak (TO), and torrefied bamboo (TB).

Methods

Elemental analysis

The elemental analysis was carried out through an elemental analyzer (EA 1108-CNHS-O, FISON Instruments, USA). All samples were instantaneously combusted in a pure oxygen atmosphere for oxidation. A quantitative analysis was carried out on C, H, N, S among the samples using a thermal conductivity detector, and O was generated by pyrolysis, transformed into CO, and redetected again through the thermal conductivity detector. The measurement was carried out three times repeatedly, and one-way analysis of variance (ANOVA) data evaluation was carried out using Duncan's new multiple range test to compare torrefied samples and untreated samples in different groups.

Ultimate analysis

The ultimate analysis was carried out through an ultimate analyzer (CKIK 5E-MACIV, Changsha Kaiyuan Instrument Co., China). The experimental conditions were to measure the moisture content at 105 °C for 1 hour. Then, it was retained for 1800 s to 750 °C for 1 h. The ash content was measured for 2 h. Lastly, the temperature was raised to 950 °C, at which temperature the volatile content was measured during 420 s. At this time, the fixed carbon content was mathematically calculated by subtracting moisture, ash, and volatile matter from the weight of the first state of each sample. The measurement and evaluation was repeated three times. Also, a one-way analysis of variance (ANOVA) data evaluation was done using Duncan's new multiple range test to compare torrefied samples and untreated samples as measured in two groups.

Thermogravimetric analysis (TGA)

Thermogravimetric analysis was performed using a TGA/DSC1 thermogravimetric analyzer (Mettler-Toledo, Greifensee, Switzerland). The gas used N_2 with a flow rate of 50 $mL \cdot min^{-1}$. The temperature increase was set to 10 $°C \cdot min^{-1}$ as a single heating rate within a temperature range of 30 to 800 °C.

Kinetic studies

Based on this theory, the basic kinetics model using TGA is generally represented by $\frac{dX}{dt}$, which is the change in the conversion rate with time at a constant temperature. Here, X is the conversion rate depending on the thermal decomposition of the sample, as expressed in Eq. 1,

$$X = \frac{W_0 - W_t}{W_0 - W_\infty} \quad (1)$$

where W_0 (g) is the initial sample weight, W_t (g) is the instantaneous sample weight, and W_∞ (g) is the final sample weight. The change in the conversion rate can be expressed as a function $f(X)$ at a constant temperature. This is the most extensively used function in polymer kinetics in which solid materials are decomposed into gaseous products. In addition, this can be expressed as Eq. 2,

$$f(X) = (1 - X)^n \quad (2)$$

where n is the order of the reaction. If pyrolysis is the n^{th} reaction, the temporal change of the conversion rate has a proportional relationship with the constant rate k, and the following equation can be established, as shown in Eq. 3,

$$\frac{dX}{dt} = kf(X) \quad (3)$$

where the constant rate k depends on the temperature, and a commonly used flammable substance under nonisothermal conditions can be expressed as follows using Arrhenius's formula, as shown in Eq. 4,

$$k = A\,exp\left(-\frac{E}{RT}\right) \quad (4)$$

where E (kJ·mol^{-1}) is activation energy, A (s^{-1}) is a pre-exponential factor, R (J·K^{-1}·mol^{-1}) is the universal gas constant, and T is the absolute temperature.

Finally, combining Eqs. 3 and 4 yields Eq. 5:

$$\frac{dX}{dt} = A\,exp\left(-\frac{E}{RT}\right)(1 - X)^n \quad (5)$$

In this study, based on Eq. 5, the differential and integral methods were used, before and after the torrefaction of the samples of each species, to obtain the parameters of the reaction kinetics.

Differential methods

Two analysis methods were used to obtain the parameters of the reaction kinetics in the differential method. Friedman's formula, which is commonly used in the thermal decomposition of solid materials, was first adopted. However, this method should be applied under multiple heating rates for a fixed conversion rate. The application of a single heating rate as a condition is not preferred. As such, in order to accurately obtain the velocity variable, it is necessary to compare the tendency fluctuation with the control group. Therefore, in the Friedman method, $n = 1$ was assumed and the obtained parameters were used as comparative data in this study. In addition, the analysis was carried out from the viewpoint of torrefied samples *versus* untreated samples and the difference between tree species among the torrefied samples. Friedman's formula can be expressed as follows, using the algebraic expression from Eq. 5 to yield Eq. 6,

$$ln\left(\frac{dX}{dt}\right) = ln[Af(X)] - \frac{E}{RT} \quad (6)$$

(Friedman 1965; Sbirrazzuoli 2007; Sbirrazzuoli 2020).

Using Eq. 6, the relationship between $\ln\left(\frac{dX}{dt}\right)$ and $\frac{1}{T}$ was established; regression analysis was performed at stage 1 and stage 2 for each sample, and E was calculated $\left(-\frac{E}{R}\right)$ (as shown in Fig. 2b).

Furthermore, the Chatterjee-Conard formula, another differential method, was adopted to calculate each parameter, substituting an arbitrary order of the reaction based on Friedman's formula with the n = 1 condition (Chatterjee and Conard 1968). Generally, it is preferable to select the order of the reaction that achieves maximum linearity when obtaining the parameters of the reaction kinetics. Moreover, it has been reported that the most suitable order of the reaction under high temperature conditions is generally less than 0.5 (Mitchell 1989; Hurt and Calo 2001; Murphy and Shaddix 2006; Murphy and Shaddix 2010). Therefore, the order of the reaction was assumed to be n = 0.1 to 0.5, and n = 1.0 was included in the comparative analysis in Friedman's formula. However, it was assumed that it follows two different order of reactions (Friedman's formula and Chatterjee-Conard's formula) simultaneously for some different reactions under arbitrarily selecting the order of reactions, respectively. Parameter A can be calculated based on ln(A) on the regression line segment (Fig. 1b) or calculated directly using exponential functions (Aktar and Adal 2019). In this study, A was obtained directly using Arrhenius's formula.

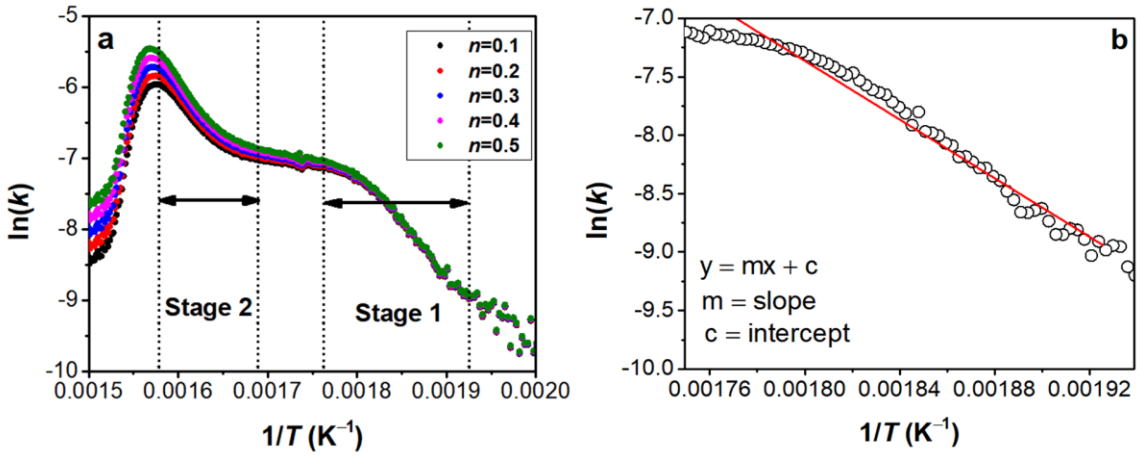

Fig. 1. Kinetic curves simulated according to the selected kinetic equation: (a) example of the kinetic parameters and analysis range for each order of the reaction; and (b) example of the kinetic parameter obtained through regression line analysis

Integral methods

For obtaining the parameters of the reaction kinetics using the integral method, the Coats-Redfern formula, which is often used in the model-fitting method and extensively used in the thermal decomposition of solid substances, was adopted (Coats and Redfern 1964). Substituting the constant heating rate $\beta = \frac{dT}{dt}$ applied in TGA (as shown in Eq. 5), resulted in Eq. 7,

$$\frac{dX}{dT} = \frac{A}{\beta} exp\left(-\frac{E}{RT}\right) f(X) \quad (7)$$

When analyzed under nonisothermal conditions, the constant heating rate β can be expressed as Eq. 8,

$$\frac{dX}{f(X)} = \frac{A}{\beta} exp\left(-\frac{E}{RT}\right) dT \quad (8)$$

On integrating Eq. 8, the following equation can be obtained, as shown in Eq. 9,

$$g(X) = \int_0^X \frac{dX}{f(X)} = \frac{A}{\beta}\int_0^T exp\left(-\frac{E}{RT}\right)\, dT \quad (9)$$

which in this case, g(X) is an integral type of reaction model.

In addition, with $T = T_0$ when $X = 0$ and $T = T_X$ when $X = X$, integration is again performed to obtain Eq. 10,

$$\int_0^X \left(\frac{1}{(1-X)^n}\right)\, dX = \int_{T_0}^{T_X} \left(\frac{A}{\beta}\right) exp\left(-\frac{E}{RT}\right) dT. \quad (10)$$

Accordingly, when $(1-X)^n$ and $exp\left(\frac{-E}{RT}\right)$ are integrated in Eq. 10, the following equation can be obtained, as shown in Eq. 11,

$$\frac{1-(1-X)^{1-n}}{1-n} = \frac{ART^2}{\beta E}\left(1-\frac{2RT}{E}\right) exp\left(-\frac{E}{RT}\right). \quad (11)$$

which, when considered as a logarithmic expression, is expressed as Eq. 12,

$$ln\left(\frac{1}{T^2}\frac{1-(1-X)^{1-n}}{1-n}\right) = ln\left(\frac{AR}{\beta E}\left(1-\frac{2RT}{E}\right)\right) - \frac{E}{R}\frac{1}{T} \quad (12)$$

Finally, if $\left(1-\frac{2RT}{E}\right) \approx 1$ is established, then Eq. 12 above can be expressed by Eq. 13 and Eq. 14,

$$ln\left(\frac{1}{T^2}\frac{1-(1-X)^{1-n}}{1-n}\right) = ln\left(\frac{AR}{\beta E}\right) - \frac{E}{R}\frac{1}{T} \qquad n \neq 1 \quad (13)$$

$$ln\left(\frac{-ln(1-X)}{T^2}\right) = ln\left(\frac{AR}{\beta E}\right) - \frac{E}{R}\frac{1}{T} \qquad n = 1 \quad (14)$$

Accordingly, the parameters of the reaction kinetics were calculated by plotting the left side, *i.e.*, (ln(*k*)) and $\frac{1}{T}$, as graphs, respectively. The slope of the parameter is $-\frac{E}{R}$ and the intercept is $ln\left(\frac{AR}{\beta E}\right)$.

Therefore, *E* and *A* can be calculated. However, for $n \neq 1$, which is the condition shown in Eq. 13, *n* was substituted assuming a range of 0.1 to 0.5 in the same manner as in the differential method described in the previous section. For $n = 1$, the calculation was performed using Eq. 14.

RESULTS AND DISCUSSION

Sample Characteristics and Chemical Compositions

Tables 1 and 2 show the elemental and chemical composition results of each specimen. In addition, as the experiments were repeated three times, statistical testing was performed to determine the significant differences among the six specimens, *i.e.*, the torrefied samples *versus* the untreated samples, through Duncan's new multiple range test. Based on the statistical results, it was confirmed that the increase in carbon elements and fixed carbon, which characterizes torrefied wood, was significantly different for the

torrefied and untreated samples (at a 99% significance). Thus, the authors attempted to determine the effect of torrefaction on woody biomass through the reaction kinetics under a single heating rate based on the premise that the chemical properties of each sample were significantly different.

Table 1. Analysis Results for Each Specimen *via* Proximate Analysis

Samples	Moisture Content (%)	DT*1	Volatile Matter (%)	DT	Ash Content (%)	DT	Fixed Carbon (%)	DT
UP*2	7.0 ± 0.1	A	82.0 ± 0.5	A	0.76 ± 0.12	A	10.3 ± 0.3	A
UO*2	7.8 ± 0.2	B	80.4 ± 1.4	A	0.64 ± 0.13	AB	11.3 ± 1.5	A
UB*2	0.5 ± 0.0	C	86.3 ± 0.3	B	1.13 ± 0.05	AB	12.1 ± 0.3	A
TP	5.7 ± 0.1	D	77.6 ± 1.6	C	1.02 ± 0.39	ABC	15.7 ± 1.2	B
TO	3.2 ± 0.1	E	75.4 ± 1.1	C	0.47 ± 0.16	BC	21.0 ± 1.2	C
TB	6.4 ± 0.1	F	71.5 ± 1.1	D	1.45 ± 0.27	C	20.7 ± 1.2	C

Note: *1 DT: Duncan's new multiple range test (*p*-value less than 0.01); and *2 Lee *et al*. 2020

Table 2. Analysis Results for Each Specimen *via* Ultimate Analysis

Samples	Carbon (%)	DT*1	Hydrogen (%)	DT	Oxygen*3 (%)	DT	Nitrogen (%)	DT
UP*2	48.59 ± 1.46	AB	6.35 ± 0.28	A	41.91 ± 0.91	BC	3.16 ± 0.27	AB
UO*2	46.57 ± 0.94	A	5.97 ± 0.38	A	44.44 ± 1.32	C	3.02 ± 0.00	AB
UB*2	49.12 ± 0.01	ABC	6.05 ± 0.05	A	42.29 ± 0.10	C	2.54 ± 0.03	A
TP	55.28 ± 0.46	D	5.79 ± 0.13	A	36.16 ± 0.25	A	2.77 ± 0.35	AB
TO	49.99 ± 0.47	BC	5.81 ± 0.04	A	41.52 ± 0.66	BC	2.68 ± 0.14	AB
TB	52.11 ± 1.01	CD	5.68 ± 0.22	A	38.86 ± 1.21	AB	3.35 ± 0.01	B

Note: *1 DT: Duncan's new multiple range test (*p*-value less than 0.01); *2 Lee *et al*. 2020; and *3 by difference

Analysis Range Selection based on TG, DTG, and D^2TG Curves

Figure 2 displays the TG reduction rate as well as the DTG and D^2TG curves. For a comparative analysis of the reaction kinetics between the torrefied and untreated samples, an analysis range was set for each sample. For example, Figs. 2a and 2b depict the parameters of oak. In the TG curve shown in Fig. 2a, it can be observed that the hemicellulose and cellulose are thermally decomposed at temperature ranges of 245 to 290 °C and 320 to 360 °C, respectively. In addition, the DTG and D^2TG curves indicated the pyrolysis of hemicellulose. The decomposition of hemicellulose can also be clearly identified through the shoulder in the DTG and D^2TG curves. Here, the regions where the hemicellulose and cellulose substantially thermally decompose are denoted as "stage 1" and "stage 2," respectively, and they were set as the analysis ranges to study the reaction kinetics.

However, as shown in Fig. 2b, the concentration of hemicellulose was considerably reduced by torrefaction, and the shoulder in graphs is not clear. Therefore, based on the section where thermal decomposition could be confirmed in the D^2TG curve, the left and right sections were divided as stages 1 and 2, respectively. Even in the pine and bamboo

samples, the shoulder could not be observed under torrefied conditions. In these cases, the analysis range was set based on the DTG and D^2TG curves, as depicted in Fig. 2b. In addition, the information on the analysis range and the TGA results for each sample is shown in Table 3.

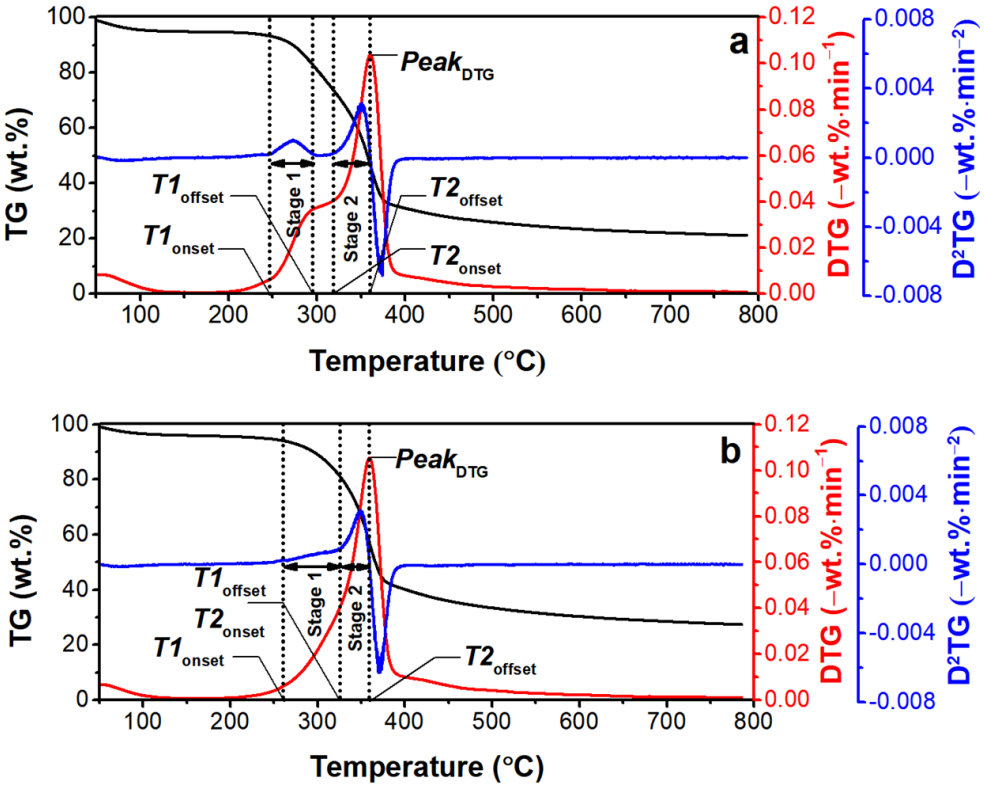

Fig. 2. Examples of the analysis range selection based on TGA and the DTG and D^2TG curves

Table 3. Analysis Results for Each Specimen Based on the TG and DTG Curves

Samples	$T1_{onset}$ (°C)	$T1_{offset}$ (°C)	$T2_{onset}$ (°C)	$T2_{offset}$ (°C)	$Peak_{DTG}$ (°C)	$Peak_{DTG}$ (-wt.%·min^{-1})	Residue (wt.%)
UP	249.47	307.41	331.75	362.17	362.20	0.085	21.70
UO	246.30	294.18	318.78	360.32	360.50	0.104	21.13
UB	223.81	292.86	310.05	348.68	348.36	0.091	23.84
TP	265.34	330.16		362.70	362.04	0.090	28.80
TO	260.58	325.66		359.26	359.22	0.105	27.40
TB	266.40	311.11		345.77	345.91	0.080	35.50

Differential Methods

Figure 3 depicts the *E* value of each species calculated under n = 1 (order of the reaction) with Friedman's formula. As shown in Fig. 1b, the activation energy *E* depends on the slope of the ln(k) parameter. Figure 3a and 3b display the results for stage 1 and stage 2, respectively. In the pyrolysis region of hemicellulose (as shown in Fig. 3a), the results of the torrefied pine and bamboo samples confirmed that there was a slight increase in the *E* value due to torrefaction (approximately +10%), whereas torrefied oak had lower *E* values, unlike the other species (-20.2%). This may be due to the higher hemicellulose content of hardwood compared to softwood and bamboo; for instance, in untreated oak hardwood, the necessary activation energy for conversion to cellulose is higher than in the untreated pine and bamboo samples (Kim *et al*. 2007).

In the pyrolysis region of cellulose (Fig. 3b), the *E* values of the torrefied oak samples were approximately 7% to 41% higher than all the other samples. Thus, it was inferred that hardwood is also affected by the thermal decomposition of cellulose because it has a relatively complex cellular structure in comparison to softwood and bamboo. Both before and after torrefaction, pine exhibited lower *E* values than the other species. In addition, the *E* value of torrefied oak was highest in the region where there is considerable cellulose thermal decomposition (+7.2% to 41.0%). Table 4 lists the values of *A* and R^2 (coefficient of determination) calculated through Friedman's formula. The R^2 value calculated for n = 1 ranged from 0.956 to 0.999, and the correlation between the regression line and ln(k) for each sample parameter was high. In the untreated group, the *A* values were higher in stage 1 compared to stage 2, except for the untreated bamboo samples. This might indicate that the number of molecular collisions per time unit generated by the thermal decomposition of hemicellulose is greater than in cellulose, and the reaction rate is faster. In the torrefied group, all the samples showed higher *A* values in stage 2 compared to stage 1. However, in the case of hardwood, the values of the torrefied oak and untreated oak samples were considerably higher compared to the other species. This may be due to the anatomical characteristics of each species rather than the effect of torrefaction.

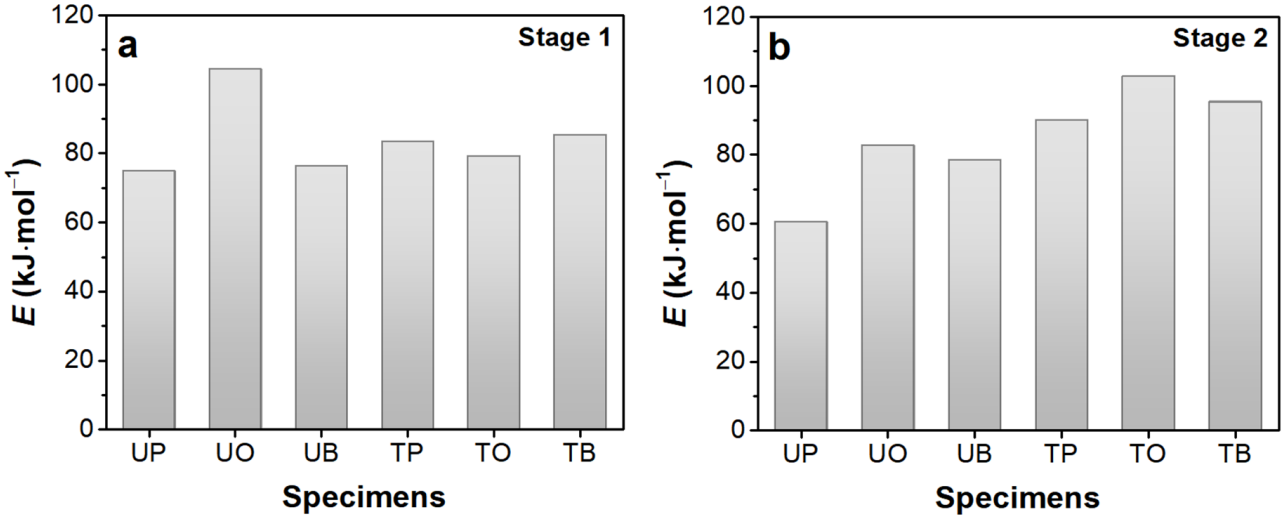

Fig. 3. Results of the activation energy (*E*) of each sample using Friedman's formula (n=1): (a) results in stage 1; and (b) results in stage 2

Table 4. Kinetic Parameters Extracted from the Differential Model Using the Friedman Method (n = 1.0)

Samples		A (s^{-1})	R^2		A (s^{-1})	R^2
Stage 1	UP	9.5E+10	0.992	Stage 2	5.7E+08	0.983
	UO	4.1E+16	0.974		1.1E+13	0.956
	UB	1.7E+11	0.987		1.4E+12	0.976
	TP	3.8E+12	0.999		2.6E+14	0.993
	TO	6.6E+11	0.997		7.4E+16	0.992
	TB	8.4E+12	0.978		2.5E+15	0.993

Figure 4 shows the E values calculated at n = 0.1 to 0.5 and 1.0, respectively, using the Chatterjee-Conard formula, and Table 5 lists the A and R^2 values. As shown in Fig. 4a, which includes the pyrolysis region of hemicellulose, the E value of the untreated pine samples was the highest for any reaction order compared to the untreated oak and untreated bamboo samples (approximately 26% to 27%) and was 18% to 23% higher than the E value of the torrefied samples.

As shown in Fig. 4b, which includes the pyrolysis region of cellulose, as the order of the reaction increased, the increase rate of the E value was higher than the rate shown in Fig. 4a, confirming that the E value of the torrefied groups was clearly higher than the E value of the untreated groups for all the species. In a study by Lee and Kim (2016), the change (decrease) in the E values of torrefied oak (treated for 300 s at 200 °C in a wood roaster) and untreated oak of the same species were approximately the same. However, the values were calculated using the model-free method at multiple heating rates, and the numerical value of the activation energy was slightly different from the one used in this study.

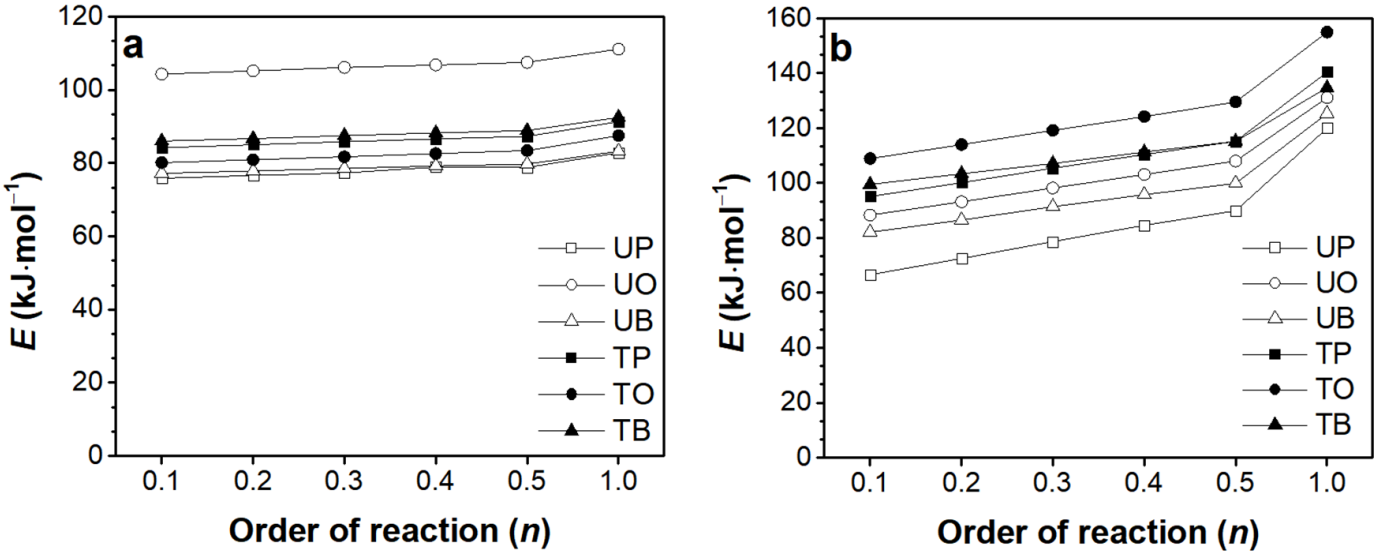

Fig. 4. Results of the activation energy of each sample using Chatterjee-Conard's method and order of the reaction condition: (a) results in stage 1; and (b) results in stage 2

Table 5. Kinetic Parameters Extracted from the Differential Model Using the Chatterjee-Conard Method

Samples		*n* = 0.1		*n* = 0.2		*n* = 0.3		*n* = 0.4		*n* = 0.5		*n* = 1.0	
		A (s^{-1})	R^2	*A* (s^{-1})	R^2	*A* (s^{-1})	R^2	*A* (s^{-1})	R^2	*A* (s^{-1})	R^2	*A* (s^{-1})	R^2
Stage 1	UP	1.5E+11	0.993	2.1E+11	0.993	2.9E+11	0.994	6.0E+11	0.994	6.0E+11	0.994	3.8E+12	0.996
	UO	4.2E+16	0.974	4.3E+16	0.975	9.6E+16	0.976	9.6E+16	0.977	1.9E+17	0.978	9.9E+17	0.981
	UB	2.7E+11	0.987	3.6E+11	0.988	4.9E+11	0.988	6.9E+11	0.988	8.7E+11	0.988	4.5E+12	0.989
	TP	5.8E+12	0.999	8.4E+12	0.999	1.2E+13	0.999	2.5E+13	0.999	2.5E+13	0.998	1.6E+14	0.965
	TO	1.0E+12	0.997	1.5E+12	0.997	2.1E+12	0.998	3.2E+12	0.998	4.6E+12	0.998	3.2E+13	0.999
	TB	1.3E+13	0.997	1.3E+13	0.997	2.5E+13	0.997	3.4E+13	0.996	4.8E+13	0.996	2.6E+14	0.996
Stage 2	UP	9.0E+09	0.984	1.3E+11	0.983	2.1E+12	0.984	3.2E+13	0.983	3.6E+14	0.982	3.1E+20	0.981
	UO	1.5E+14	0.957	1.6E+14	0.956	1.3E+16	0.956	1.3E+16	0.955	1.2E+18	0.955	5.0E+22	0.951
	UB	7.6E+12	0.974	5.8E+13	0.973	5.5E+14	0.974	4.1E+15	0.973	2.7E+16	0.972	2.9E+21	0.973
	TP	2.6E+15	0.995	9.0E+12	0.996	2.8E+17	0.997	2.2E+19	0.998	2.3E+19	0.998	2.1E+24	0.994
	TO	1.2E+18	0.992	1.2E+19	0.992	1.3E+20	0.992	1.2E+21	0.991	1.4E+22	0.990	1.4E+27	0.986
	TB	1.7E+16	0.998	1.8E+16	0.998	5.4E+17	0.998	3.6E+18	0.998	2.1E+19	0.998	1.5E+23	0.997

Moreover, it was confirmed that the value of ln(*k*) of the differential method calculated in this study is more sensitive to the thermal decomposition of cellulose, which suggested that the reaction rate to heat varies considerably depending on the species or biomass material.

In addition, the parameter values calculated using Friedman's formula ($n = 1$) were most similar to those calculated at $n = 0.2$. The correlation relationship and trend between the two differential methods for the *E* value are consistent ($R^2 = 1.000$ and $R^2 = 0.994$ for stages 1 and 2, respectively). As shown in Fig. 2a, the higher the order of the reaction, the greater the deviation from the peak at approximately 0.0015 to 0.0016 K^{-1}. Furthermore, it was confirmed that the range of the thermal decomposition peak of cellulose in stage 2 (Fig. 2) was slightly out-of-range compared to that lower concentration of cellulose from the DTG and D^2TG curves.

For the samples under all the conditions, the *E* value showed a tendency to gradually increase as the order of the reaction increases from $n = 0.1$ to 0.5. For $n = 1.0$, the values were approximately 33% to 44% higher on average. As shown in Table 5, the R^2 values of the parameters for calculating *E* and *A* had a relationship of 0.951 to 0.999 for all the samples. The *A* values in stage 1, as well as stage 2, increased as the order of the reaction increased, but the rate of increase was considerably higher in stage 2. The number of molecular collisions in the torrefied oak and untreated oak samples, which are hardwoods, were considerably higher than the number of molecular collisions in other the species.

Integral method

Figure 5 depicts the *E* values in stage 1 and stage 2 calculated using the Coats-Redfern formula. The results of the integral method differed from the results of the differential method. As shown in Fig. 5a, the results for the untreated oak samples were the same those obtained using the Friedman and Chatterjee-Conard differential methods, and the torrefied oak samples exhibited almost the same trend (the average of $n = 0.1$ to 0.5 was 40.9 kJ mol^{-1} and $n = 1.0$ was 40.4 kJ mol^{-1}, respectively). The *E* values of the torrefied pine and untreated bamboo samples, in particular, were approximately 37.7 and 37.6 kJ mol^{-1} on average, respectively, and overlapped with each other on the graph. The average value of the torrefied bamboo samples was 34.9 kJ mol^{-1}, while the average value of the untreated pine samples was 32.5 kJ mol^{-1}. The untreated group exhibited a clear trend: untreated oak was greater than untreated bamboo, which was greater than untreated pine. In the torrefied group, torrefied oak was greater than torrefied pine, which was greater than torrefied bamboo. Figure 5b shows a clear separation between the results of the untreated group (the average of $n = 0.1$ to 0.5 and 1.0 was 50.6 kJ mol^{-1}) and the torrefied group (the average of $n = 0.1$ to 0.5 and 1.0 was 75.5 kJ mol^{-1}). In addition, there was no significant difference in the results of each species. For all of the three species, the *E* value of the torrefied group was approximately 33% higher than the *E* value of the untreated group. Accordingly, it was also confirmed that the ln(*k*) value of the integral method calculated in this study was more sensitive to the thermal decomposition of cellulose, similar to the ln(*k*) value calculated using the differential method.

Table 6 shows the R^2 value of each parameter, including *E* and *A* calculated using the Coats-Redfern formula. The correlation of the parameters for all the samples was in the 0.957 to 0.999 range. In addition, the number of molecular collisions was less than those of the Friedman and Chatterjee-Conard differential methods (10^{14} to 10^{15}).

Table 6. Kinetic Parameters Extracted from the Integral Model Using the Coats-Redfern Method

Samples		*n* = 0.1		*n* = 0.2		*n* = 0.3		*n* = 0.4		*n* = 0.5		*n* = 1.0	
		A (s^{-1})	R^2	*A* (s^{-1})	R^2	*A* (s^{-1})	R^2	*A* (s^{-1})	R^2	*A* (s^{-1})	R^2	*A* (s^{-1})	R^2
Stage 1	UP	3.8E+14	0.975	3.8E+14	0.974	3.9E+14	0.974	3.9E+14	0.974	3.9E+14	0.973	4.2E+14	0.971
	UO	4.8E+14	0.965	4.9E+14	0.964	4.9E+14	0.963	4.9E+14	0.961	4.9E+14	0.963	5.2E+14	0.963
	UB	4.4E+14	0.960	4.4E+14	0.960	4.5E+14	0.959	4.5E+14	0.959	4.6E+14	0.959	4.8E+14	0.957
	TP	4.4E+14	0.969	4.5E+14	0.969	4.5E+14	0.968	4.5E+14	0.968	4.6E+14	0.967	4.8E+14	0.966
	TO	4.7E+14	0.977	4.7E+14	0.977	4.8E+14	0.977	4.8E+14	0.976	4.9E+14	0.976	5.2E+14	0.974
	TB	4.1E+14	0.980	4.1E+14	0.979	4.1E+14	0.980	4.2E+14	0.979	4.3E+14	0.979	4.4E+14	0.978
Stage 2	UP	5.4E+14	0.999	5.7E+14	0.998	6.0E+14	0.998	6.2E+14	0.997	6.6E+14	0.997	8.2E+14	0.994
	UO	5.2E+14	0.988	5.5E+14	0.987	5.7E+14	0.986	5.9E+14	0.985	6.2E+14	0.983	7.6E+14	0.976
	UB	5.2E+14	0.991	5.4E+14	0.991	5.7E+14	0.990	5.9E+14	0.989	5.6E+14	0.992	7.4E+14	0.982
	TP	8.4E+14	0.998	8.7E+14	0.998	9.0E+14	0.997	9.2E+14	0.997	9.5E+14	0.997	1.1E+15	0.994
	TO	8.2E+14	0.995	8.4E+14	0.994	8.8E+14	0.994	9.0E+14	0.993	9.3E+14	0.992	1.1E+15	0.988
	TB	8.2E+14	0.997	8.4E+14	0.996	8.6E+14	0.996	8.8E+14	0.996	9.1E+14	0.995	1.0E+15	0.993

The method of calculating the pre-exponential factor for each reaction kinetics formula was completely different between the differential and integral methods. Therefore, between the two, the most reliable analysis method cannot be determined. As shown in Fig. 2, it would be most appropriate to analyze using the values that have the closest tendency to the results confirmed by the TG, DTG, and D^2TG curves. All the equations should be combined to select the conditions that comprehensively match the properties of each sample. Moreover, as shown in Table 6, in the untreated group, an equal or slight increase was confirmed for the response order of the reaction, *i.e.*, n = 0.1 to 0.5 and 1.0, whereas a gradual increase was confirmed in the torrefied group. Interestingly, even with the integration method, the number of molecular collisions of the untreated oak sample in stage 1 was the highest among all the samples, which was consistent with the results of the differential methods. However, in stage 2, the deviation between the untreated and torrefied groups was relatively large, as depicted by the E values. Furthermore, it is worth nothing that the lowest value of the untreated pine samples was recorded in stage 1, whereas the highest was recorded in stage 2.

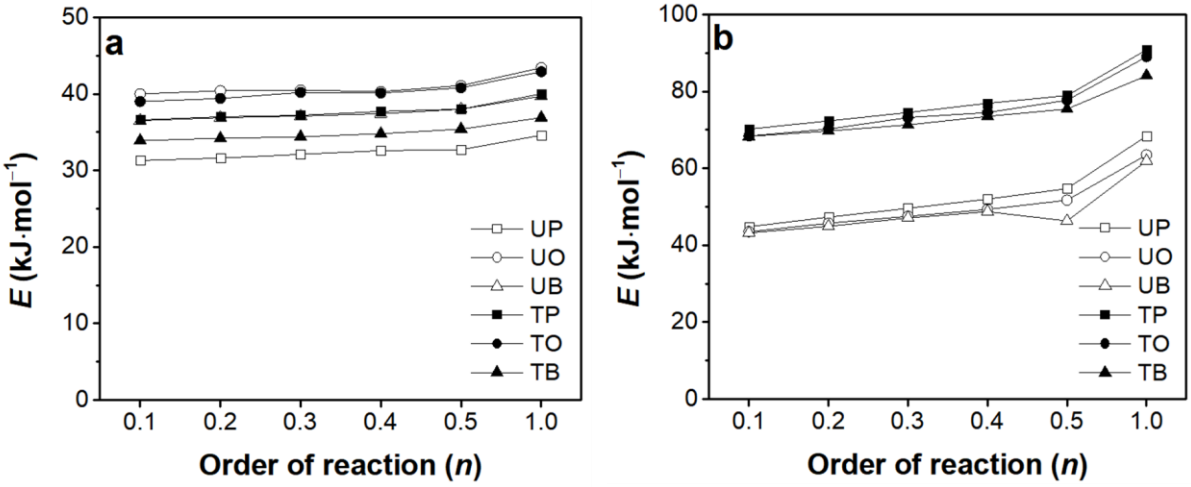

Fig. 5. Results of the activation energy for each sample using the Coats-Redfern method and the order of the reaction condition: (a) results in stage 1; and (b) results in stage 2

To finally evaluate the thermal degradation behavior and kinetics in the bulk state of the sample using the results discussed above, the average values (apparent activation energy and apparent pre-exponential factor) of all the parameters for n = 0.1 to 0.5 and n=1.0 were calculated using the two differential methods and the integral method for each species and treatment condition, respectively. The comparison of the results, with respects to the species and treatment conditions, is presented in Table 7.

According to the results averaged using each formula, the energy required for the thermal decomposition of "moisture + volatile matter → hemicellulose" and "hemicellulose → cellulose" was common among the three species. Pine, which is softwood, was found to be the most effective solid fuel material. Moreover, as the torrefied sample was in a state in which moisture and a certain amount of volatile matter have been removed through the pre-treatment at approximately 200 °C, torrefied pine had a higher calorific value than the untreated sample. As per the results reported by Lee *et al*. (2016), torrefied pine, torrefied oak, and torrefied bamboo have a higher calorific value, 5499, 4992, and 5200 $kcal \cdot kg^{-1}$, respectively.

Table 7. Evaluation Results of Each Kinetic Method

Samples	Friedman		Chatterjee-Conard		Coats-Redfern	
	E (kJ·mol^{-1})	*A* (s^{-1})	*E* (kJ·mol^{-1})	*A* (s^{-1})	*E* (kJ·mol^{-1})	*A* (s^{-1})
UP	67.8	4.8E+10	81.9	2.6E+19	42.6	5.13E+14
UO	93.7	2.1E+16	105.2	4.2E+21	45.6	5.48E+14
UB	77.4	7.9E+11	88.0	2.4E+20	43.2	5.20E+14
TP	86.7	1.3E+14	99.4	1.8E+23	57.5	6.93E+14
TO	91.1	3.7E+16	103.9	1.2E+26	58.0	6.98E+14
TB	90.4	1.3E+15	100.1	1.3E+22	54.3	6.53E+14

Based on the results of *E* and *A* in this study, it was determined that torrefied pine had the fastest ignition. All the parameters of the kinetics formula for torrefied bamboo and torrefied oak were proximate to each other (particularly, the pre-exponent factor). According to the research results of Panshin and Zeeuw (1980), the chemical composition of bamboo is similar to that of softwood (40% to 52%) and hardwood (38% to 56%) with a glucan content of approximately 40% to 48% (hemicellulose and cellulose). The lignin content is approximately 25% to 30%, and it can be seen that the chemical composition of bamboo is similar to that of softwood (24% to 37%) and hardwood (17% to 30%). As bamboo is abundant in minerals compared to softwood, it has properties that are relatively close to hardwood.

A related article by Mehdi *et al*. (2021) reported that the mass (wt%) and energy yield of solid fuel according to the increase in temperature of torrefaction process was higher than hardwood (wood pellet). This suggests that softwoods in woods have a shorter combustion time than hardwoods. This may be unsuitable for products that require a long combustion time, such as molded charcoal, except for wood pellets. Therefore, a considerable quantity of inorganic matter was present even after torrefaction. The combustion rate of bamboo (both untreated and torrefied bamboo) was lower than the combustion rate of softwood. The ash content (Table 1) was also higher than in the other species, supporting the results shown in Fig. 3b. However, as a solid fuel, fuel with a long combustion time after ignition will be superior to torrefied oak and torrefied bamboo raw materials, which had a higher fixed carbon amount compared to torrefied pine (approximately 24% to 25%). In future research on torrefied biomass, it will be necessary to analyze in detail the processing costs incurred in the torrefaction process and classification based on utilization.

CONCLUSION

1. According to the analysis of the region where the major components (hemicellulose and cellulose) of each sample were considerably thermally decomposed, under the model-fitting method using the kinetics formula of the differential (Friedman, Chatterjee-Conard) and integral (Coats-Redfern) methods at a single heating rate (10 °C·min^{-1}), certain numerical differences were observed. However, the trends exhibited by the parameters of all the samples were consistent.

2. When *n* (order of reaction) was less than or equal to 0.5, the experiment was carried out based on the assumption that it is a suitable condition to obtain the activation energy (*E*) and pre-exponential energy factor (*A*) kinetically, but no unique results or trends were confirmed except for numerical difference. However, as the order of the reaction increased, it was confirmed that the peak, which was set within the temperature range (K^{-1}) of the samples based on the DTG and D^2TG curves, gradually moved away. Therefore, it is necessary to carefully observe the variable order of reaction in order to obtain the correct parameters for each major chemical compound of wood cell wall by thermal decomposition.
3. According to the results of the kinetic analysis in this study, softwood was the most reactive and required less activation energy, *i.e.*, the minimum energy required for the section where the major chemical components of each species are pyrolyzed. In addition, considering that the carbon content and fixed carbon content were high due to torrefaction, softwood may be used as a solid fuel with a fast ignition and high reactivity, *e.g.*, wood pellets, *etc*.), but it has a lower carbon content than hardwood or bamboo, *e.g.*, briquettes, *etc*.). However, it may be unsuitable as a raw material due to its short combustion time. Therefore, selection of the appropriate species for fuel production based on the required application is suggested.

ACKNOWLEDGMENTS

This study was carried out with the support of R&D Program for Forest Science Technology (Project No. 2018117B10-2020-AB01) provide by Korea Forest Service (Korea Forestry Institute).

REFERENCES CITED

Aktar, T., and Adal, E. (2019). "Determining the Arrhenius kinetics of avocado oil: Oxidative stability under Rancimat test conditions," *Foods* 8(7), 1-13. DOI: 10.3390/foods8070236

Bach, Q.-V., and Tran, K.-Q. (2015). "Dry and wet torrefaction of woody biomass-a comparative study on combustion kinetics," *Energy Procedia* 75, 150-155. DOI: 10.1016/j.egypro.2015.07.270

Carrier, M., Auret, K., Bridgwater, A. and Knoetze, J. H. (2016). "Using apparent activation energy as a reactivity criterion for biomass pyrolysis," *Energy Fuels* 30(10), 7834-7841. DOI: 10.1021/acs.energyfuels.6b00794

Chatterjee, P. K., and Conard, C. M. (1968). "Thermogravimetric analysis of cellulose," *Journal of Polymer Science Part A: Polymer Chemistry* 6(12), 3217-3233. DOI: 10.1002/pol.1968.150061202

Chen, C., Ma, X., and He, Y. (2012). "Co-pyrolysis characteristics of microalgae *Chlorella vulgaris* and coal through TGA," *Bioresource Technology* 117, 264-273. DOI: 10.1016/j.biortech.2012.04.077

Chen, D., Gao, A., Cen, K., Zhang, J., Cao, X., and Ma, Z. (2018). "Investigation of biomass torrefaction based on three major components: Hemicellulose, cellulose, and

lignin," *Energy Conversion and Management* 169, 228-237. DOI: 10.1016/j.enconman.2018.05.063

Chen, W.-H., Lin, B.-J., Lin, Y.-Y., Chu, Y.-S., Ubando, A. T., Show, P. L., Ong, H. C., Chang, J.-S., Ho, S.-H., Culaba, A. B., *et al.* (2021). "Progress in biomass torrefaction: Principle, applications and challenge," *Progress in Energy and Combustion Science* 82, 1-34. DOI: 10.1016/j.pecs.2020.100887

Coats, A. W. and Redfern, J. P. (1964). "Kinetic parameters from thermogravimetric data," *Nature* 201, 68-69. DOI: 10.1038/201068a0

El-Sayed, S. A., and Mostafa, M. E. (2014). "Pyrolysis characteristics and kinetic parameters determination of biomass fuel powders by differential thermal gravimetric analysis (TGA/DTG)," *Energy Conversion and Management* 85, 165-172. DOI: 10.1016/j.enconman.2014.05.068

El-Sayed, S.A., and Mostafa, M.E. (2015). "Kinetic parameters determination of biomass pyrolysis fuels using TGA and DTA techniques," *Waste and Biomass Valorization* 6, 401-415. DOI: 10.1007/s12649-015-9354-7

Friedman, H. L. (1965). "Kinetics of thermal degradation of char-forming plastics from thermogravimetry. Application to a phenolic plastic," *Journal of Polymer Science Part C: Polymer Symposia* 6(1), 183-195. DOI: 10.1002/polc.5070060121

Gaitán-Álvarez, J., Moya, R., Puente-Urbina, A., and Rodriguez-Zúñiga, A. (2018). "Thermogravimetric, devolatilization rate, and differential scanning calorimetry analyses of biomass of tropical plantation species of Costa Rica torrefied at different temperatures and times," *Energies* 11(4), 1-26. DOI: 10.3390/en11040696

Hurt, R. H., and Calo, J. M. (2001). "Semi-global intrinsic kinetics for char combustion modeling," *Combustion and Flame* 125(3), 1138-1149. DOI: 10.1016/50010-2180(01)00234-6

Idris, S. S., Rahman, N. A., Ismail, K., Alias, A. B., Rashid, Z. A., and Aris, M. J. (2010). "Investigation on thermochemical behaviour of low rank Malaysian coal, oil palm biomass and their blends during pyrolysis *via* thermogravimetric analysis (TGA)," *Bioresource Technology*101(12), 4584-4592. DOI: 10.1016/j.biortech.2010.01.059

Jang, E.-S., Song, E., Yoon, J., and Kim, Y.-M. (2020). "Kinetic analysis for the pyrolysis of solid refuses fuel using livestock manure," *Applied Chemistry for Engineering* 31(4), 443-451. DOI: 10.14478/ace.2020.1047

Kim, D.-Y., Kang, S.-H., and Jeong, H. (2007). "A study on pyrolytic and anatomical characteristics of Korean softwood and hardwood," *Journal of the Korean Wood Science and Technology* 35(6), 31-42.

Lee, C., Choi, C., Yoo, J., Kim, H., Yang, S., and Kang, S. (2016). "The combustion characteristics of self-igniting briquettes prepared with torrefied wood power from a wood-roasting method," *BioResources* 11(4), 9803-9810. DOI: 10.15376/biores.11.4.9803-9810

Lee, C.-G., Kim, M.-J., and Eom, C.-D. (2020). "A study on pyrolysis characteristics and fuel performance of major forest biomass feedstock," *Korean Forest Bioenergy* 30(2), 1-7. DOI: 10.37581/KFB.220.12.30.2.1

Lee, D., and Kim, B.-J. (2016). "A study on the thermal properties and activation energy of rapidly torrefied oak wood powder using non-isothermal thermogravimetric analysis," *Journal of Korean Wood Science and Technology* 44(1), 96-105. DOI: 10.5658/WOOD.2016.41.1.96

Mamvura, T. A., and Danha, G. (2020). "Biomass torrefaction as an emerging technology to aid in energy production," *Heliyon* 6(3), 1-17. DOI: 10.1016/j.heliyon.2020.e03531

Mehdi, R., Raza, N., Naqvi, S. R., Khoja, A.H., Mehran, M. T., Farooq, M., and Tran, K. Q. (2021). "A comparative assessment of solid fuel pellets production from torrefied agro-residues and their blends," *Journal of Analytical and Applied Pyrolysis* 156, 105125. DOI:10.1016/j.jaap.2021.105125

Mitchell, R. E. (1989). "On the products of the heterogeneous oxidation reaction at the surface of burning coal char particles," *Symposium (International) on Combustion* 22(1), 69-78. DOI: 10.1016/S0082-0784(89)80012-8

Murphy, J. J., and Shaddix, C. R. (2006). "Combustion kinetics of coal chars in oxygen-enriched environments," *Combustion and Flame* 144(4), 710-729. DOI: 10.1016/j.combustflame.2005.08.039

Murphy, J. J., and Shaddix, C. R. (2010). "Effect of reactivity loss on apparent reaction order of burning char particles," *Combustion and Flame* 157(3), 535-539. DOI: 10.1016/j.combustflame.2009.09.013

Panshin, A. J., and Zeeuw, C. D. (1980). *Textbook on Wood Technology: Structure, Identification, Properties, and Uses of the Commercial Woods of the United States and Canada*, McGraw-Hill, New York, NY.

Phanphanich, M., and Mani, S. (2011). "Impact of torrefaction on the grindability and fuel characteristics of forest biomass," *Bioresource Technology* 102(2), 1246-1253. DOI: 10.1016/j.biortech.2010.08.028

Prins, M. J., Ptasinski, K. J., and Janssen, F. J. (2006). "Torrefaction of wood: Part 2. Analysis of products," *Journal of Analytical and Applied Pyrolysis* 77(1), 35-40. DOI: 10.1016/j.jaap.2006.01.001

Rana, S., Parikh, J. K., and Mohanty, P. (2013). "Thermal degradation and kinetic study for different waste/rejected plastic materials," *Korean Journal of Chemical Engineering* 30(3), 626-633. DOI: 10.1007/s11814-012-0157-2

Ren, S., Lei, H., Wang, L., Bu, Q., Chen, S., and Wu, J. (2013). "Thermal behaviour and kinetic study for woody biomass torrefaction and torrefied biomass pyrolysis by TGA," *Biosystems Engineering* 116(4), 420-426. DOI: 10.1016/j.biosystemseng.2013.10.003

Saldarriaga, J. F., Aguado, R., Pablos, A., Amutio, M., Olazar, M., and Bilbao, J. (2015). "Fast characterization of biomass fuels by thermogravimetric analysis (TGA)," *Fuel* 140, 744-751. DOI: 10.1016/j.fuel.2014.10.024

Sbirrazzuoli, N. (2007). "Is the Friedman method applicable to transformations with temperature dependent reaction heat?," *Macromolecular Chemistry and Physics* 208(14), 1592-1597. DOI: 10.1002/macp.200700100

Sbirrazzuoli, N. (2020). "Determination of pre-exponential factor and reaction mechanism in a model-free way," *Thermochimica Acta* 691, 1-16. DOI: 10.1016/j.tca.2020.17807

Stelt, M. J. C. v. d., Gerhauser, H., Kiel, J. H. A., and Ptasinski, K. J. (2011). "Biomass upgrading by torrefaction for the production of biofuels: A review," *Biomass and Bioenergy* 35(9), 3748-3762. DOI: 10.1016/j.biombioe.2011.06.023

Vyazovkin, S., and Wight, C. A. (1999). "Model-free and model-fitting approaches to analysis of isothermal and nonisothermal data," *Thermochimica Acta* 340-341, 53-68. DOI: 10.1016/S0040-6031(99)00253-1

Article submitted: August 13, 2021; Peer review completed: October 9, 2021; Revised version received and accepted: November 15, 2021; Published: November 22, 2021.
DOI: 10.15376/biores.17.1.411-428